1993

Angular and radial correlation in doubly excited systems when 1 ≤ Z ≤ 4. The 2p2 3P state

D. R. T. Keeble

K. E. Banyard

Gordon W. F. Drake
University of Windsor

Angular and radial correlation in doubly excited systems when 1<or=Z<or=4: the $2p^2\ ^3P$ state

1993 J. Phys. B: At. Mol. Opt. Phys. 26 2811

(http://iopscience.iop.org/0953-4075/26/17/015)

J. Phys. B: At. Mol. Opt. Phys. 26 (1993) 2811–2825. Printed in the UK

Angular and radial correlation in doubly excited systems when $1 \leqslant Z \leqslant 4$: the $2p^2\ ^3P$ state

D R T Keeble†, K E Banyard† and G W F Drake‡

† Department of Physics and Astronomy, University of Leicester, Leicester, LE1 7RH, UK
‡ Department of Physics, University of Windsor, Windsor, Ontario, Canada

Received 11 January 1993

Abstract. The angular and radial components of electron correlation have each been examined in detail for the discrete $2p^2\ ^3P$ states of H^-, He, Li^+ and Be^{2+}. These doubly excited sytems were described by highly accurate explicitly correlated wavefunctions. The analysis involved the use of angular Coulomb holes, changes in the one- and two-particle radial density distributions and several angular and radial expectation values. Additionally, various statistical correlation coefficients were used which emphasized, in turn, angular and radial correlation properties in different regions of the two-particle density.

The angular holes and related properties showed a clearly defined inverse-Z effect for He and the positive ions. This trend was not repeated for the radial curves. However, the radial densities did reveal a distinct 'in-out' correlation effect—similar in character to the split-shell behaviour for the ground state. By comparison with the findings for $Z \geqslant 2$, the angular and radial correlation effects for H^- were always exceedingly large, thus setting it apart from the other systems. For He, the angular hole for the comparatively slow moving $2p^2\ ^3P$ electrons was found to be over 50% deeper than that for the ground state and about six times the depth of a $1s2p\ ^3P$ hole. The statistical correlation coefficients highlighted a steady growth, with Z, in the relative importance of angular correlation. Nevertheless, for each system, these coefficients indicated that the radial effect was the prevailing influence on the two-particle probability distribution.

1. Introduction

By comparison with the gound state, doubly excited states (DES) of simple atoms are occupied by relatively slow moving electrons and, consequently, they should be more responsive to the influence of Coulomb correlation. This was demonstrated to be the case for the $2p^2\ ^3P$ states of H^-, He, Li^+ and Be^{2+} by Banyard *et al* (1992, hereafter referred to as BKD). In that work, we analysed the correlation-induced changes in the probability distribution for r_{12}, the interelectronic separation, by means of Coulomb holes, partial Coulomb holes and various $\langle r_{12}^n \rangle$. Comparisons were made with the ground state and the singly-excited state $1s2p\ ^3P$. The latter comparison arose since, for low Z, an important decay mechanism for the $2p^2\ ^3P$ state is by a radiative transition to the $1s2p\ ^3P$ level. It is observed that, being discrete, the $2p^2\ ^3P$ state exhibits no wavefunction mixing with open channels. Transitions involving this DES have been considered by, for example, Westerveld *et al* (1979), Auderbert *et al* (1984) and Karim and Bhalla (1988). See our previous report (BKD) for further references.

In the present article, we perform an in-depth appraisal of the separate angular and radial components of electron correlation associated with the $2p^2\ ^3P$ state when $1 \leqslant Z \leqslant 4$. As before, the correlated descriptions are provided by the highly accurate

0953-4075/93/172811+15$07.50

wavefunctions of Drake (1986); the non-correlated reference state is again represented by the restricted Hartree-Fock (HF) functions obtained from a program by Froese-Fischer (1987). In addition to reporting angular Coulomb holes and correlation-induced changes in the one- and two-particle radial densities, we also determine a series of expectation values and calculate various statistical correlation coefficients τ (see Kutzelnigg *et al* 1968 and, more recently, Banyard and Mobbs 1981, and Thakkar 1987). Atomic units are used throughout this work.

Other studies of either angular or radial correlation, or both, for simple systems in excited states have been undertaken by many workers. Some typical references are Sinanoğlu and Herrick (1975), Rehmus *et al* (1978), Ezra and Berry (1983), Nicolaides *et al* (1987), Ojha and Berry (1987), Dmitrieva and Plindov (1988), Rau and Molina (1989), Ivanov (1992) and Chen *et al* (1992).

2. Calculations and results

Drake (1986) wrote the space part of the explicitly correlated wavefunction for the $He(2p^2\ ^3P)$-like systems as

$$\Psi_{corr}(r_1, r_2) = (1 - P_{12}) \sum_{i,j,k}^{N} A_{ijk} r_1^i r_2^j r_{12}^k \exp(-\alpha r_1 - \beta r_2)\, Y^{M=1}_{l_1=1,l_2=1,L=1}(\theta_1, \phi_1, \theta_2, \phi_2)$$

where

$$Y^{M=1}_{l_1=1,l_2=1,L=1}(\theta_1, \phi_1, \theta_2, \phi_2) = 2^{-1/2}[\, Y^1_1(\theta_1, \phi_1)\, Y^0_1(\theta_2, \phi_2) - Y^0_1(\theta_1, \phi_1)\, Y^1_1(\theta_2, \phi_2)]. \quad (1)$$

P_{12} is a permutation operator and, as shown, the angular term involves products of spherical harmonic functions. A summary of the remaining notation is given in BKD. Since N is the upper limit on the summation, it is used to designate a particular wavefunction. As previously, we examine two correlated wavefunctions for each Z: the energetically best function and, for comparison, the function with the fewest terms. For H^-, the Drake wavefunction with least terms has $N = 20$ and recovers 99.72% of the correlation energy. All other Drake functions describing the $1 \leqslant Z \leqslant 4$ systems yielded percentages in *excess* of that obtained by the D-20 (Drake: equation (1) with $N = 20$) wavefunction for H^-. N values, total energies E and correlation percentages are quoted in table 1 of BKD. Each numerical HF wavefunction, HF(NUM), derived from the Froese-Fischer (1987) program is represented by the same linear combination of Slater-type orbitals (STO) as used before. These fitted HF(STO) functions are employed throughout this work but, for comparison, expectation values are reported for both HF(NUM) and HF(STO).

Following Youngman and Banyard (1987), the distribution function for $\gamma = \theta_{12}$, the angle between the position vectors r_1 and r_2 for the two electrons, is given in terms of a normalized space wavefunction $\Psi(r_1, r_2)$ by

$$P(\gamma) = \int \Psi^*(r_1, r_2)\Psi(r_1, r_2)\, d\tau_1\, d\tau_2/d\gamma \quad (2)$$

where, unlike an earlier definition by Banyard and Ellis (1972), we note that

$$\int_0^{\pi} P(\gamma)\, d\gamma = 1. \quad (3)$$

The origin of coordinates is always located at the nucleus; see figure 1 of BKD (1992) where, in that instance, the inter-vector angle was labelled θ_{12}. The angular Coulomb hole is defined here as

$$\Delta P(\gamma) = P_{\text{corr}}(\gamma) - P_{\text{HF}}(\gamma) \tag{4}$$

where the integral of $\Delta P(\gamma)$ with respect to $0 \leqslant \gamma \leqslant \pi$ is zero. For the $2p^2\,{}^3P$ state

$$P_{\text{HF}}(\gamma) = \tfrac{3}{4}\sin^3(\gamma). \tag{5}$$

The plot of $P_{\text{HF}}(\gamma)$ is shown in figure 1A along with the $\Delta P(\gamma)$ curves for H^- derived from the D-20 and D-84 correlated wavefunctions. In figure 1B, we show the angular holes associated with the energetically best Drake functions: D-84 for H^- and D-70 for He, Li^+ and Be^{2+}. For each $Z \geqslant 2$, the correlated wavefunction with the fewest terms, D-13, produced a $\Delta P(\gamma)$ curve which was graphically indistinguishable from that for the D-70 function. Figure 2 shows the curves for $1 \leqslant Z \leqslant 4$ when scaled to give $Z\Delta P(\gamma)$ against γ. In figure 3 the angular hole for He is compared with the corresponding

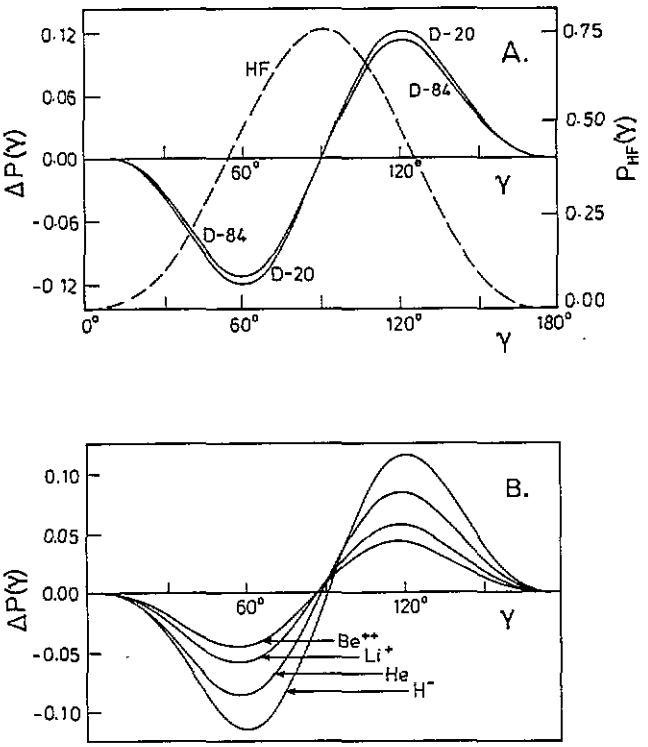

Figure 1. A: the normalized angular function $P_{\text{HF}}(\gamma)$ for all Hartree-Fock (HF) $2p^2\,{}^3P$ *wavefunctions;* γ *is the angle subtended by electrons 1 and 2 at the nuclear origin. Also* shown are the angular Coulomb holes, $\Delta P(\gamma) = P_{\text{corr}}(\gamma) - P_{\text{HF}}(\gamma)$, for $H^-(2p^2\,{}^3P)$. The $P_{\text{corr}}(\gamma)$ functions are derived from the Drake wavefunction in equation (1) using, in turn, $N = 20$ and $N = 84$. The $\Delta P(\gamma)$ curves are denoted by their correlated descriptions D-20 and D-84.

B: the $\Delta P(\gamma)$ *curves for the* $2p^2\,{}^3P$ *state when* $1 \leqslant Z \leqslant 4$. For each system, $P_{\text{corr}}(\gamma)$ is obtained from the energetically best version of equation (1): the D-84 wavefunction for H^- and the D-70 versions for He, Li^+ and Be^{2+}. When $Z \geqslant 2$, the D-13 functions yielded $\Delta P(\gamma)$ curves which were graphically indistinguishable from the corresponding D-70 curve.

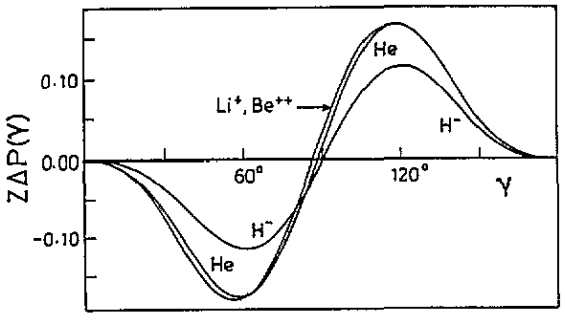

Figure 2. The Z-scaled angular holes for the $2p^2\,{}^3P$ states of H^-, He, Li^+ and Be^{2+} using the energetically best correlated wavefunctions: D-84 for H^- and the D-70 functions when $Z \geqslant 2$.

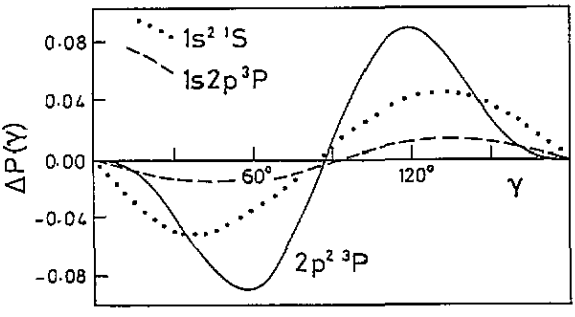

Figure 3. Comparison of the angular holes, $\Delta P(\gamma)$ against γ, for the $2p^2\,{}^3P$, $1s2p\,{}^3P$ and $1s^2\,{}^1S$ states of He. The full curve is for the $2p^2\,{}^3P$ state, the broken curve and the dotted curve represent the $1s2p\,{}^3P$ and $1s^2\,{}^1S$ states, respectively. For this order of these He states, the correlated descriptions are provided by the energetically best wavefunctions of Drake (1986), Tweed (1973) and Weiss (1961).

results for the $1s^2\,{}^1S$ and $1s2p\,{}^3P$ states taken, respectively, from Banyard and Ellis (1972) and (1975). Their angular Coulomb curves for both states have been revised to satisfy equations (2) and (3). The correlated description of the ground state was provided by a 35-term configuration-interaction (CI) wavefunction (Weiss 1961) which recovered 98.8% of the correlation energy whereas, for the singly excited state, they used an explicitly correlated wavefunction (Tweed 1973) which accounted for 78.6% of the correlation energy.

As usual, the normalized radial distribution is defined as

$$D(r_1) = \int \Psi^*(\boldsymbol{r}_1, \boldsymbol{r}_2)\Psi(\boldsymbol{r}_1, \boldsymbol{r}_2)\, \mathrm{d}\tau_1\, \mathrm{d}\tau_2/\mathrm{d}r_1 \tag{6}$$

and, hence, we formed a one-particle radial hole

$$\Delta D(r_1) = D_{\mathrm{corr}}(r_1) - D_{\mathrm{HF}}(r_1). \tag{7}$$

Similarly, a two-particle radial function can be expressed as

$$D(r_1, r_2) = \int \Psi^*(\boldsymbol{r}_1, \boldsymbol{r}_2)\Psi(\boldsymbol{r}_1, \boldsymbol{r}_2)\, \mathrm{d}\tau_1\, \mathrm{d}\tau_2/\mathrm{d}r_1\, \mathrm{d}r_2 \tag{8}$$

and the corresponding correlation change is given by

$$\Delta D(r_1, r_2) = D_{\text{corr}}(r_1, r_2) - D_{\text{HF}}(r_1, r_2). \tag{9}$$

Obviously we have

$$\int_0^\infty \int_0^\infty \Delta D(r_1, r_2)\, dr_1\, dr_2 = \int_0^\infty \Delta D(r_1)\, dr_1 = 0. \tag{10}$$

When plotted against Zr_1, figure 4A shows $Z^{-1}D_{\text{HF}}(r_1)$ for each Z and figure 4B shows $\Delta D(r_1)$ for $2 \leqslant Z \leqslant 4$ (the H^- curve is omitted because of its size, see figure 5). In each instance, the correlated description used in forming $\Delta D(r_1)$ is derived from the energetically best Drake wavefunction. Included in figure 4A, as a broken curve, is the radial distribution generated from an independent-particle $2p^2\,{}^3P$ wavefunction

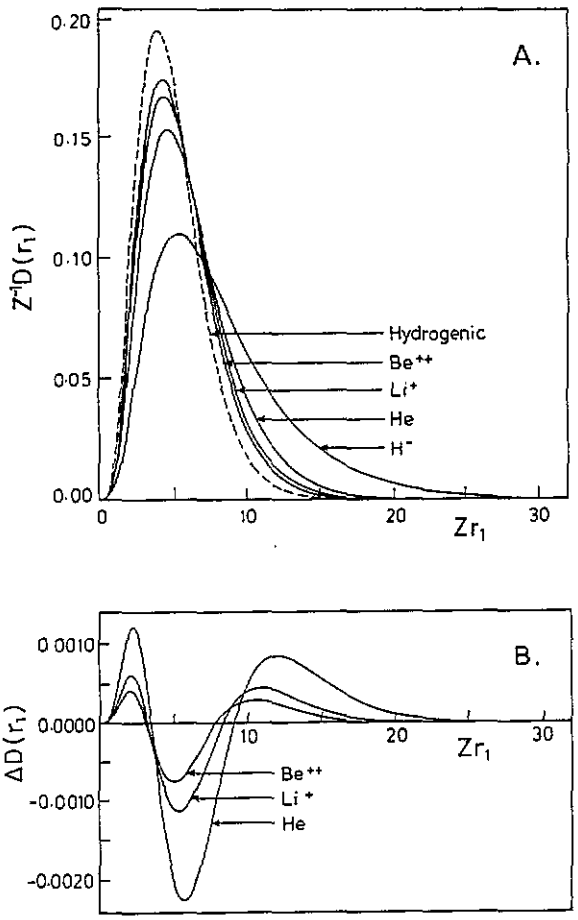

Figure 4. A: radial densities $D_{\text{HF}}(r_1)$ derived from the HF wavefunctions for the $2p^2\,{}^3P$ states when $1 \leqslant Z \leqslant 4$. The broken curve is $D(r_1)$ generated from an independent-particle $2p^2\,{}^3P$ wavefunction comprising unoptimized hydrogenic orbitals. Both axes are scaled to preserve normalization.

B: correlation-induced changes in the one-particle density, $\Delta D(r_1)$, for He, Li^+ and Be^{2+} plotted against Zr_1. For each system, a D-70 correlated wavefunction is used to determine $D_{\text{corr}}(r_1)$ in equation (7).

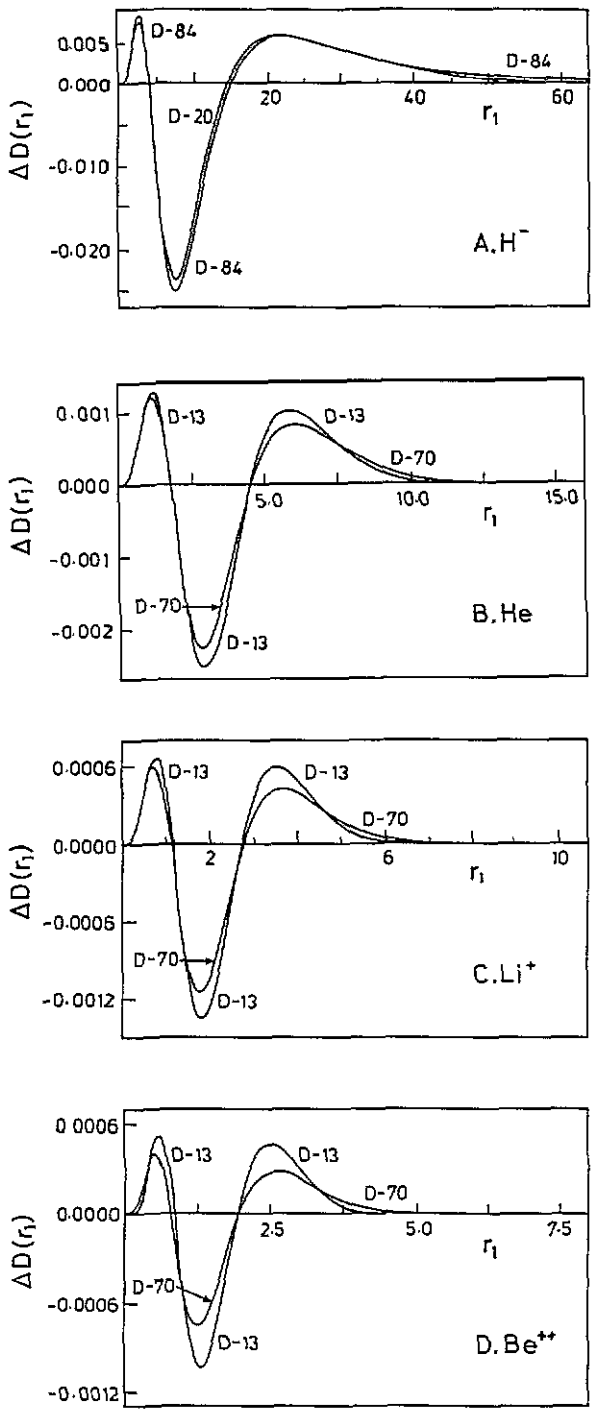

Figure 5. Comparisons of $\Delta D(r_1)$ for the $2p^2\,{}^3P$ state of H^-, He, Li^+ and Be^{2+} using, in each case, two energetically different correlated wavefunctions; see the diagrams A–D, respectively. For $Z=1$, results for $\Delta D(r_1)$ are shown when $D_{corr}(r_1)$ in equation (7) is derived, in turn, from the correlated D-20 and D-84 wavefunctions. For each $Z \geqslant 2$, the $\Delta D(r_1)$ curves correspond to the appropriate D-13 and D-70 correlated functions.

based on unoptimized hydrogenic orbitals. The $\Delta D(r_1)$ curves arising from the two versions of equation (1) for each system are compared in figure 5, as indicated. The $D_{HF}(r_1, r_2)$ and $\Delta D(r_1, r_2)$ functions are shown as surfaces in figure 6 for H^- and He; $D_{corr}(r_1, r_2)$ in equation (9) was obtained from D-84 for H^- and D-70 for He. Since the results for Li^+ and Be^{2+} differ, essentially, only in scale from those for He, they are not included in figure 6.

The expectation values $\langle r_1^n r_2^n \cos\gamma\rangle$, $\langle r_1^n\rangle$ and $\langle r_1^n r_2^n\rangle$ for these $2p^2\,{}^3P$ states are given in tables 1–3, where n is an integer. $\langle\gamma\rangle$, obtained from $P(\gamma)$, is quoted in table 1 and the standard deviation σ for each $D(r_1)$ is given in table 2. For each Z, tables 2 and 3 contain values derived from HF(NUM) and its HF(STO) representation. The correlation-induced changes in $P(\gamma)$ and $D(r_1)$ can also be assessed by evaluating

$$\Upsilon_\gamma = \tfrac{1}{2}\int_0^\pi |\Delta P(\gamma)|\,\mathrm{d}\gamma \text{ and } \Upsilon_r = \tfrac{1}{2}\int_0^\infty |\Delta D(r_1)|\,\mathrm{d}r_1. \tag{11}$$

The results for Υ_γ and Υ_r, expressed as percentages of the integrated HF distributions, are given in tables 1 and 2. In addition, defining the change in a statistical correlation coefficient as $\Delta\tau = \tau(\text{corr}) - \tau(\text{HF})$, we determined $\Delta\tau_{1/r}$, $\Delta\tau_r$, $\Delta\tau_{\gamma'}$, $\Delta\tau_{\gamma''}$ and $\Delta\tau_\gamma$. Definitions of these radial and angular τ, involving $\langle r_1^n r_2^n\rangle$ and $\langle r_1^n r_2^n \cos\gamma\rangle$ respectively, have been quoted recently by Banyard (1990), see equations (1)–(5). For radial correlation, $\Delta\tau_{1/r}$ places the emphasis on the *inner* regions of the two-particle density in position space whereas $\Delta\tau_r$ locates the emphasis in the outer regions of the density. Similarly, when discussing angular correlation, we note that $\Delta\tau_{\gamma'}$, $\Delta\tau_{\gamma''}$ and $\Delta\tau_\gamma$ possess, in that order, an emphasis which moves progressively from the *inner* to the *outer* regions of the two-particle density. The values are presented in table 4.

3. Discussion

3.1. Angular correlation

For a $2p^2\,{}^3P$ state, the $P_{HF}(\gamma)$ curve in figure 1A is applicable for any Z. Since the two electrons singly occupy, say, the $2p_0$ and $2p_1$ orbitals at the independent-particle level, the inter-electronic angular distribution is symmetric about its maximum. Hence in table 1, $\langle\gamma\rangle = 90°$ for the HF descriptions. Naturally, the $\sin\gamma$ term arising from the Jacobian and contained, by implication, in the definition of $P(\gamma)$, see equation (2), renders the distribution function zero when $\gamma = 0°$ or 180° for *any* state.

As we progress from the D-20 to the D-84 wavefunction for H^-, the correlation energy is improved by 0.27%. Figure 1A shows that this improvement is reflected in $\Delta P(\gamma)$. Although the crossover points are virtually coincident at about 90°, the energetically better curve (D-84) is seen to be not quite so deep in the $0 < \gamma < 90°$ region and, consequently, it is less positive when $90° < \gamma < 180°$. As found for $P_{HF}(\gamma)$, each angular Coulomb hole in figure 1 is effectively zero at small γ; a similar behaviour occurs as $\gamma \to 180°$.

When $Z \geqslant 2$, the D-13 wavefunction recovers over 99.9% of the correlation energy and the use of the D-70 function improves the result by $\leqslant 0.08\%$. Therefore, for He and the positive ions, it is not surprising that the two $\Delta P(\gamma)$ curves are indistinguishable to within graphical accuracy: see figure 1B. For general comparison, figure 1B includes the H^-(D-84) curve. Table 1 reveals that the *introduction* of correlation produces a

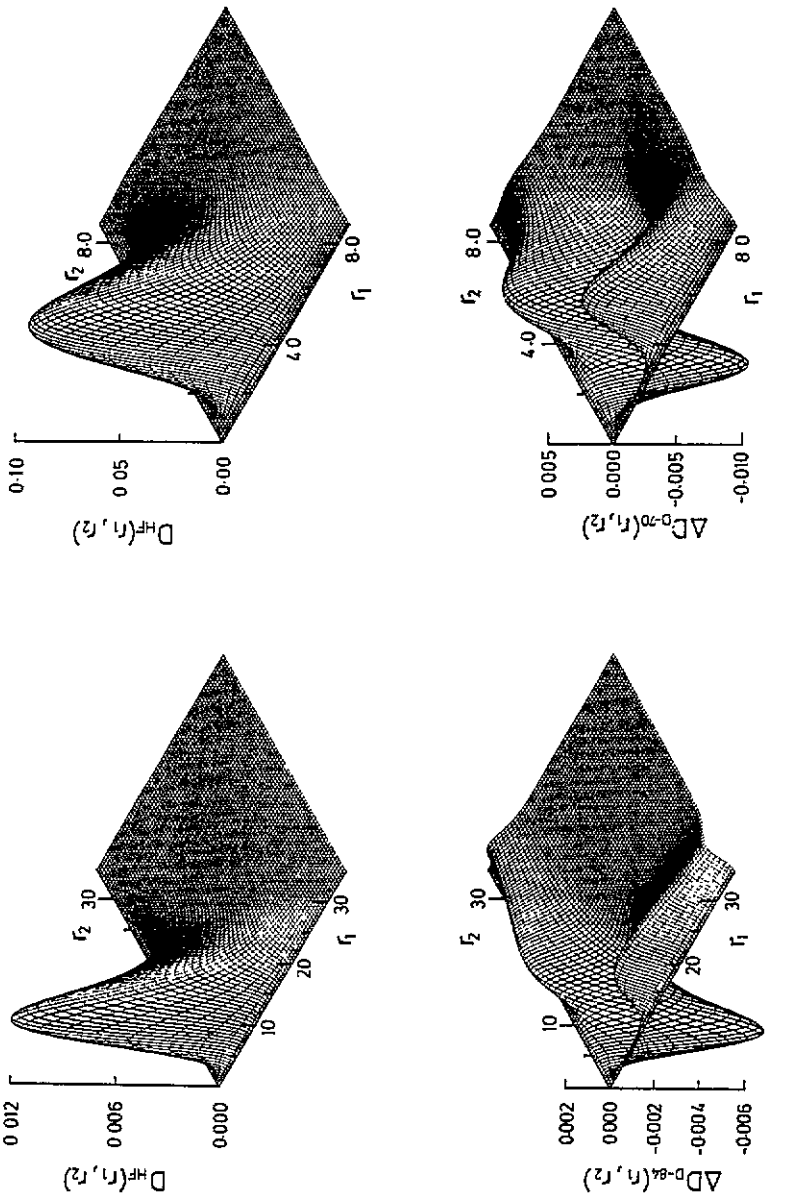

Figure 6. The correlation-induced change $\Delta D(r_1, r_2)$ in the two-particle radial density and the HF-based distribution $D_{HF}(r_1, r_2)$ for the $2p^2\,{}^3P$ states of H^- and He. $D_{corr}(r_1, r_2)$ in equation (9) is derived from D-84 for H^- and D-70 for He. Results are not shown for Li^+ and Be^{2+} since, except for changes of scale, the characteristics of the surfaces are similar to those for He.

Table 1. Expectation values $\langle r_1^n r_2^n \cos\gamma\rangle$ and $\langle\gamma\rangle$ for the He($2p^2\,{}^3P$)-like systems when $1 \leq Z \leq 4$, where $n = -1$, 0, +1, and γ is the angle subtended by the position vectors r_1 and r_2 at the nucleus as origin. Υ_γ is the percentage of the normalized probability function $P_{HF}(\gamma)$ redistributed due to electron correlation. Throughout this work, all distances are measured in atomic units.

System	Wavefunction[a]	$\langle r_1^{-1} r_2^{-1} \cos\gamma\rangle$	$\langle\cos\gamma\rangle$	$\langle r_1^{+1} r_2^{+1} \cos\gamma\rangle$	$\langle\gamma\rangle$ (deg)	Υ_γ (%)
$H^-(2p^2\,{}^3P)$	D-20[b]	−0.001 9780	−0.097 966	−7.712 7	96.200	9.18
	D-84	−0.001 9176	−0.094 344	−7.383 3	95.971	8.84
$He(2p^2\,{}^3P)$	D-13	−0.010 331	−0.071 449	−0.744 38	94.528	6.66
	D-70	−0.010 299	−0.071 404	−0.743 10	94.526	6.65
$Li^+(2p^2\,{}^3P)$	D-13	−0.017 932	−0.048 310	−0.195 94	93.065	4.49
	D-70	−0.017 890	−0.048 287	−0.195 54	93.064	4.49
$Be^{2+}(2p^2\,{}^3P)$	D-13	−0.025 560	−0.036 378	−0.077 893	92.310	3.37
	D-70	−0.025 494	−0.036 363	−0.077 804	92.308	3.38

[a] Hartree–Fock (HF) values for $\langle r_1^n r_2^n \cos\gamma\rangle$ are zero in each instance. We also note that $\langle\gamma\rangle_{HF} = 90°$.
[b] D-20, for example, refers to the Drake (1986) wavefunction with $N = 20$ in the summation limit in equation (1).

Table 2. Values of $\langle r_1^n\rangle$ for the $2p^2\,{}^3P$ states when $1 \leq Z \leq 4$ and $-2 \leq n \leq +2$. Also quoted is σ, the radial standard deviation, and Υ_r, the percentage of the normalized density $D_{HF}(r_1)$ which is redistributed due to electron correlation.

System	Wavefunction	$\langle r_1^{-2}\rangle$	$\langle r_1^{-1}\rangle$	$\langle r_1^{+1}\rangle$	$\langle r_1^{+2}\rangle$	σ	Υ_r(%)
$H^-(2p^2\,{}^3P)$	HF (NUM)	0.041 392	0.167 31	8.3220	92.467	4.817 7	—
	HF (STO)	0.041 388	0.167 29	8.3243	92.530	4.820 3	—
	D-20	0.043 008	0.161 54	10.804	199.22	9.083 0	14.2
	D-84	0.042 999	0.160 67	11.481	251.16	10.925	15.3
$He(2p^2\,{}^3P)$	HF (NUM)	0.240 82	0.417 90	3.0814	11.691	1.481 7	—
	HF (STO)	0.240 82	0.417 90	3.0814	11.691	1.481 7	—
	D-13	0.241 70	0.418 10	3.0895	11.782	1.495 8	0.404
	D-70	0.241 72	0.418 10	3.0899	11.791	1.497 9	0.378
$Li^+(2p^2\,{}^3P)$	HF (NUM)	0.606 97	0.667 95	1.9043	4.4165	0.888 92	—
	HF (STO)	0.606 97	0.667 95	1.9043	4.4166	0.888 93	—
	D-13	0.607 65	0.668 05	1.9057	4.4258	0.891 18	0.130
	D-70	0.607 68	0.668 05	1.9058	4.4271	0.891 74	0.114
$Be^{2+}(2p^2\,{}^3P)$	HF (NUM)	1.139 8	0.917 96	1.3786	2.3045	0.635 60	—
	HF (STO)	1.139 8	0.917 96	1.3786	2.3045	0.635 59	—
	D-13	1.140 3	0.918 02	1.3790	2.3066	0.636 27	0.0691
	D-70	1.140 3	0.918 02	1.3791	2.3071	0.636 54	0.0530

noticeable increase in $\langle\gamma\rangle$ for each system, particularly for H^-. However, the *improvement* in the correlated wavefunctions discussed above is seen to cause a reduction in $\langle\gamma\rangle$ for H^- of about 0.23° whereas, for He, Li^+ and Be^{2+}, the decrease is only marginal. We also note that, for each system, the quantum mechanical results for $\langle\gamma\rangle$ and the angular probability distributions $P_{HF}(\gamma)$ and $\Delta P(\gamma)$ lend support to the quasiclassical picture of a $2p^2\,{}^3P$ state as being a floppy linear 'triatomic molecule', see Krause *et al* (1987). This molecular model of electron correlation, initially proposed by Herrick and Kellman (1980), assumes that the two electrons are localized diametrically at equal

Table 3. Values of $\langle r_1^n r_2^n \rangle$ for the $2p^2\,{}^3P$ states when $1 \leq Z \leq 4$ and $-2 \leq n \leq +2$.

System	Wavefunction	$\langle r_1^{-2} r_2^{-2} \rangle$	$\langle r_1^{-1} r_2^{-1} \rangle$	$\langle r_1^{+1} r_2^{+1} \rangle$	$\langle r_1^{+2} r_2^{+2} \rangle$
$H^-(2p^2\,{}^3P)$	HF (NUM)	0.001 7133	0.027 991	69.256	8549.5
	HF (STO)	0.001 7129	0.027 987	69.294	8561.8
	D-20	0.000 786 24	0.020 255	85.210	11 596
	D-84	0.000 766 24	0.019 757	91.951	14 727
$He(2p^2\,{}^3P)$	HF (NUM)	0.057 994	0.174 64	9.4952	136.67
	HF (STO)	0.057 994	0.174 64	9.4952	136.67
	D-13	0.050 515	0.168 82	9.2444	122.83
	D-70	0.050 595	0.168 83	9.2471	123.08
$Li^+(2p^2\,{}^3P)$	HF (NUM)	0.368 41	0.446 15	3.6264	19.506
	HF (STO)	0.368 41	0.446 15	3.6264	19.506
	D-13	0.339 71	0.437 58	3.5676	18.303
	D-70	0.340 02	0.437 60	3.5680	18.323
$Be^{2+}(2p^2\,{}^3P)$	HF (NUM)	1.299 1	0.842 64	1.9006	5.3109
	HF (STO)	1.299 1	0.842 64	1.9006	5.3109
	D-13	1.227 2	0.831 25	1.8785	5.0789
	D-70	1.227 3	0.831 26	1.8786	5.0800

Table 4. Changes due to correlation in various statistical correlation coefficients τ for the $2p^2\,{}^3P$ states when $1 \leq Z \leq 4$. $\Delta\tau_{1/r}$ and $\Delta\tau_r$ assess the radial component of correlation and $\Delta\tau_{\gamma'}$, $\Delta\tau_{\gamma^*}$ and $\Delta\tau_\gamma$ assess the angular component. For each component, the chosen $\Delta\tau$ represent a progressive shift of emphasis from the inner to the outer regions of the two-particle probability distribution. We note that, since τ(HF) is zero for these systems, each $\Delta\tau = \tau$(corr).

System	Wavefunction	$\Delta\tau_{\gamma'}$	$\Delta\tau_{\gamma^*}$ [a]	$\Delta\tau_\gamma$	$\Delta\tau_{1/r}$	$\Delta\tau_r$
$H^-(2p^2\,{}^3P)$	D-20	−0.045 99	−0.097 97	−0.038 71	−0.345 3	−0.382 0
	D-84	−0.044 60	−0.094 34	−0.029 40	−0.352 4	−0.334 0
$He(2p^2\,{}^3P)$	D-13	−0.042 74	−0.071 45	−0.063 18	−0.089 44	−0.134 3
	D-70	−0.042 61	−0.071 40	−0.063 02	−0.089 28	−0.133 8
$Li^+(2p^2\,{}^3P)$	D-13	−0.029 51	−0.048 31	−0.044 27	−0.053 96	−0.080 60
	D-70	−0.029 44	−0.048 29	−0.044 17	−0.053 87	−0.080 37
$Be^{2+}(2p^2\,{}^3P)$	D-13	−0.022 42	−0.036 38	−0.033 77	−0.038 65	−0.057 45
	D-70	−0.022 36	−0.036 36	−0.033 72	−0.038 69	−0.057 51

[a] We note that $\tau_{\gamma^*} = \langle \cos\gamma \rangle$. The definition of each τ used here has been quoted recently by Banyard (1990), equations (1-5).

distances from the nucleus: the system then experiences quantized collective rotations and large bending vibrations. Ezra and Berry (1983) have used this model to examine, in detail, a 'molecular' interpretation of the dynamics of correlation in various DES for a series of He-like ions. Of particular interest is their comment that the $2p^2\,{}^3P$ state can be regarded as a floppy molecule with one quantum of bending vibration. Figure 7 of Ezra and Berry (1983) shows that their conditional probability density for the $2p^2\,{}^3P$ state has a maximum around $\gamma = 90°$ and, because of symmetry constraints, possesses nodes at $\gamma = 0°$ and 180°. More importantly, however, they observe that, in the region when r_1 equals the most probable value for r_2, angular correlation shifts

the maximum in the density to values of γ which are slightly greater than 90°. As Z was increased, Ezra and Berry (1983) found that the conditional probability density tended to become more symmetric about $\gamma = 90°$.

The simple Z-scaling employed here in figure 2 for the angular holes produces a near-coincidence over the whole range, except of course for H^-. Clearly, even though $\Delta P(\gamma)$ for H^- has the largest magnitude in figure 1B, the angular hole is too small to fit in with the inverse-Z behaviour observed here. When $Z \geqslant 2$, the inverse-Z effect is also shown in the Y_γ values and in the *excess* of the correlated $\langle\gamma\rangle$ values over the HF result of 90°, see table 1 in each case. For He, the comparison in figure 3 of the angular hole for $2p^2\ ^3P$ with those for the $1s2p\ ^3P$ and $1s^2\ ^1S$ states reveals large differences in magnitude, the curves being ordered as DES> ground state > singly excited state. Indeed, the DES hole is over 50% deeper than the $1s^2\ ^1S$ hole and several times deeper than that for $1s2p\ ^3P$. Nevertheless, we note that the value for γ which *locates* the minimum in each curve increases according to the occupancy of a p orbital. Such an ordering is not applicable to the crossover or nodal point where, as figure 3 shows, the $1s2p\ ^3P$ curve has the largest γ value. However, in a study of angular holes for the ground state (Banyard and Ellis 1972), it was found that a wavefunction which recovered about 80% of the correlation energy produced a nodal point with a γ value larger than that obtained when the description was over 95% correlated. Thus, for the $1s2p\ ^3P$ state, the use of a correlated wavefunction which is less accurate than those for the other states may have yielded a nodal γ which is, in reality, too large. Obviously, for He, the differences between these curves are sufficiently large to conclude that angular correlation has a much greater effect on the slow moving DES electrons than on the $1s^2\ ^1S$ or $1s2p\ ^3P$ electrons, in spite of the diffuse nature of the DES charge cloud.

3.2. Radial correlation

When examining the influence of correlation on the radial distributions $D(r_1)$ and $D(r_1, r_2)$, defined in equations (6) and (8), respectively, it is to be expected that the one-particle function $D(r_1)$ will be less sensitive than $D(r_1, r_2)$. In figure 4A, the $D(r_1)$ curves have been Z-scaled in such a way that normalization is preserved. The curves for $1 \leqslant Z \leqslant 4$, derived from the HF(STO) results, are observed to converge towards $D(r_1)$ generated from an independent-particle $2p^2\ ^3P$ wavefunction using unoptimized hydrogenic orbitals. As in BKD, this confirms the *decreasing* importance of the interelectronic repulsion term as Z increases. In figure 4B, the $\Delta D(r_1)$ against Zr_1 curves obtained from the energetically best correlated wavefunctions show a roughly common *form* when $Z \geqslant 2$. The curve for H^- is not included due to its extensive r_1 range *and* the comparatively massive magnitude for $\Delta D(r_1)$, see figure 5. The 'double-occupancy' of the 2p orbital, with its non-zero angular momentum, is seen to produce curves for $D_{HF}(r_1)$ and $\Delta D(r_1)$ which have negligible values at small r_1. By contrast, the HF curves for $1s^2\ ^1S$ and $1s2p\ ^3P$, each involving a 1s orbital, are known to rise rapidly from the origin. An attempt was made to reduce the ranges of the cross over regions in figure 4B by using a $(Z - k)$ scaling factor. Unfortunately, the screening parameter $k = 0.28$ required for a minimized spread of inner nodes was quite different from that of 0.49 required for the outer nodes.

For each system, the radial 'in-out' effect of correlation is immediately apparent. Like the 'split-shell' effect for the $1s^2\ ^1S$ state, a $\Delta D(r_1)$ curve is seen to be most negative at a Zr_1 value slightly in excess of that for the maximum in the corresponding $D_{HF}(r_1)$: we also note that each set of Zr_1 values approaches a limit as Z increases. Obviously,

as Z becomes larger, $\Delta D(r_1)$ decreases in magnitude and relative importance. This is supported by the Y_r values in table 2 where the *decrease* with Z is considerably greater than that observed for Y_γ in table 1.

In figure 5, the $\Delta D(r_1)$ curves for H^- show a distinction between the D-20 and D-84 correlated wavefunctions and, for He and the positive ions, differences exist between results derived from the D-13 and D-70 functions. As expected, for these pairs of highly correlated wavefunctions the differences, although real, are indeed very small when compared with $D_{HF}(r_1)$. Nevertheless, figure 5 shows that the improvement in the correlated wavefunction for H^- deepens the radial hole and makes $\Delta D(r_1)$ more extensive. For $Z \geqslant 2$, improvement again extends each curve but the hole is *less* deep than that for D-13.

Examination of the two-particle radial densities in figure 6 reveals that the relatively massive correlation effect for H^- extends well beyond the region of the $D_{HF}(r_1, r_2)$ surface. For He, $\Delta D(r_1, r_2)$ is almost confined within the (r_1, r_2) range for the HF surface, a feature which was clearly apparent when comparing the surfaces for Li^+ and for Be^{2+} (the pairs of surfaces for $Z = 3$ and 4 are not shown for reasons of space). The 'in-out' effect is highlighted in $\Delta D(r_1, r_2)$ by a maximum being located at small r_2 and large r_1, and vice versa, coupled with the occurrence of a reduction in probability whenever $r_1 = r_2$.

3.3. Expectation values and $\Delta\tau$

Table 1 shows that, in keeping with $\langle\gamma\rangle_{corr}$ being greater than $\langle\gamma\rangle_{HF} = 90°$, the introduction of correlation produces a negative value for the angular-related properties $\langle r_1^n r_2^n \cos\gamma\rangle$. For each system, the magnitude of the value when $n = +1$ is several times larger than the result when $n = 0$ or -1: in fact, for H^-, we note that in relative terms the size of $\langle r_1^{+1} r_2^{+1} \cos\gamma\rangle$ is extremely large. When Z is increased, $\langle r_1^{+1} r_2^{+1} \cos\gamma\rangle$ decreases rapidly in magnitude but, as mentioned, it remains the dominant value—in spite of $\langle r_1^{-1} r_2^{-1} \cos\gamma\rangle$ becoming steadily more negative. Improvement in the correlated wavefunctions is seen to decrease the magnitude of each expectation value for all Z, thus indicating a reduction in angular correlation, as observed earlier.

In table 2, correlation increases $\langle r_1^n\rangle$ and σ for He and the positive ions. For H^-, a noticeable reduction occurs for the energy-related property $\langle r_1^{-1}\rangle$, but all other quantities are increased. Indeed, the change in $\langle r_1^{+2}\rangle$ for H^- is over *two*fold and reflects the sizeable 'in-out' radial effect discussed above. When $Z \geqslant 2$, going from D-13 to D-70 is seen to yield a marginal or zero increase in $\langle r_1^n\rangle$ and a slight increase in σ. However, improving the correlated description for H^- causes a *significant* increase in $\langle r_1^{+1}\rangle$, $\langle r_1^{+2}\rangle$ and σ.

The $\langle r_1^n r_2^n\rangle$ values in table 3 show a marked sensitivity to correlation effects. Except when $n = +1$ and $+2$ for H^-, all quantities are reduced in value by the use of the explicitly correlated wavefunctions: as might be anticipated, the reduction decreases with increasing Z. When $Z \geqslant 2$, these changes relative to the HF values range from a reduction of almost 13% down to about $4\frac{1}{2}$%. However, when $Z = 1$, correlation produces a massive 55% reduction for $\langle r_1^{-2} r_2^{-2}\rangle$ and an *increase* of around 36% for $\langle r_1^{+2} r_2^{+2}\rangle$. Excluding H^-, the use of the energetically better correlated functions produces either a small or quite marginal increase in $\langle r_1^n r_2^n\rangle$. For H^-, the use of the D-84 description, instead of D-20, causes a decrease when $n \leqslant -1$ and an increase when $n \geqslant +1$, the result for $\langle r_1^{+2} r_2^{+2}\rangle$ being changed by 27%. In passing, we note from tables 2 and 3 the high degree of similarity between the HF(NUM) values and those derived from its HF(STO)

representation. Not surpisingly, the slightly reduced quality of the fitted function implied by the results for H^- is a reflection of the very diffuse nature of its $2p^2\,{}^3P$ wavefunction.

All statistical correlation coefficients considered in table 4 are identically zero when derived from an HF wavefunction as, indeed, they are for *any independent-particle* representation of $2p^2\,{}^3P$. Hence, $\Delta\tau = \tau(\text{corr})$. Since, by definition, every τ is bounded between -1 and $+1$, these different measures of angular and radial correlation are therefore capable of intercomparison: we recall that -1 and $+1$ correspond to perfect negative and positive correlation, respectively. When $Z \geqslant 2$, table 4 reveals that the angular quantities $\Delta\tau_{\gamma''}$ and $\Delta\tau_{\gamma}$ (emphasizing, in turn, the interemdiate and outer regions of the density) are always of larger magnitude than $\Delta\tau_{\gamma'}$ (emphasizing the inner regions of density). The largest value for H^- is $\Delta\tau_{\gamma''}$. For each system, the radial quantities $\Delta\tau_{1/r}$ and $\Delta\tau_r$ are seen to be greater than the angular $\Delta\tau$; this is especially so for H^- where both sets of radial values are greater by at least a factor of 3.5. Once more, this highlights the distinctive importance of radial correlation in the description of $H^-(2p^2\,{}^3P)$.

Further interest in table 4 arises from the *ratios* of various $\Delta\tau$ and, in particular, their Z-dependent trends. For example, the ratio $\Delta\tau_r/\Delta\tau_{1/r}$ is 0.95, 1.50, 1.49 and 1.49 for H^-, He, Li^+ and Be^{2+}, respectively, showing that the balance of *radial* correlation at different distances from the nucleus is similar in the neutral and positive systems, but is again distinct for H^-. When ordered as before, the angular ratio of the outer to the inner effect, $\Delta\tau_{\gamma}/\Delta\tau_{\gamma'}$, yields 0.66, 1.48, 1.50 and 1.51. Thus, when $Z \geqslant 2$, the relative strengths of *angular* correlation in different radial regions of the density are seen to be almost constant. Moreover, from the quite remarkable similarity between these two sets of ratios, we conclude that, for each system except H^-, the relative measure of the angular effects is virtually *equal* to that for the radial effects. By contrast, the ratios for H^- are seen to be significantly different. It is also informative to examine the ratio of a radial to an angular $\Delta\tau$. For increasing Z, $\Delta\tau_{1/r}/\Delta\tau_{\gamma'}$ is 7.90, 2.10, 1.83 and 1.73 and $\Delta\tau_r/\Delta\tau_{\gamma}$ is 11.4, 2.12, 1.82 and 1.71. Hence, we note that, in both the inner and outer regions of space, angular correlation becomes relatively more important as Z increases. The change in going from H^- to He is seen to be quite dramatic in both regions. Nevertheless, for each Z, these ratios suggest that radial correlation remains, overall, the prevailing influence on the two-particle probability density.

Generally, the improvement in these correlated wavefunctions causes a decrease in magnitude for the listed $\Delta\tau$, the exceptions being $\Delta\tau_{1/r}$ for H^- and $\Delta\tau_{1/r}$ and $\Delta\tau_r$ for Be^{2+} which, as seen from table 4, become more negative.

4. Summary

Highly accurate explicitly correlated wavefunctions, of benchmark quality, have been used to examine angular and radial correlation effects in the doubly excited state $2p^2\,{}^3P$ when $1 \leqslant Z \leqslant 4$. Following our recent article on the total correlation effect, these separate components of electron correlation are assessed here in terms of an angular Coulomb hole, a radial hole, several expectation values and various angular and radial statistical correlation coefficients.

For He and the positive ions, a clearly defined inverse-Z relationship exists for the angular holes $\Delta P(\gamma)$ against γ, where γ is the inter-electronic angle subtended at the nucleus. Naturally, this behaviour also occurs in Υ_γ: the overall change caused by

correlation in the normalized angular distribution $P(\gamma)$. In addition, the Z-effect is reflected in the difference between the correlated and Hartree–Fock (HF) expectation values for γ. Although H^- possesses much the largest angular hole in absolute terms, the curve is still too small to form part of the inverse-Z pattern; a similar conclusion holds for Υ_γ and the correlation-induced excess for $\langle\gamma\rangle$. For He, the curve for the doubly excited state was compared with the angular holes for the $1s^2\,{}^1S$ and $1s2p\,{}^3P$ states. The $2p^2\,{}^3P$ state, with its diffuse probability density and relatively slow moving electrons, was found to have an angular hole which is noticeably *greater* than that for each energetically lower state.

The influence of correlation on the one-particle radial density $D(r_1)$ reveals a marked 'in–out' effect which parallels the correlated 'split-shell' behaviour of the doubly occupied ground state. By analogy with the angular behaviour, the size of the radial hole $\Delta D(r_1)$ for H^- is much larger than that obtained for each of the other systems. However, irrespective of the H^- result, no simple Z-scaling effect could bring the remaining $\Delta D(r_1)$ curves into any overall agreement. For the two-particle radial function $D(r_1, r_2)$, the outward redistribution caused by correlation for H^- extends well beyond the (r_1, r_2)-range observed for $D_{HF}(r_1, r_2)$. For each system, the maxima in $\Delta D(r_1, r_2)$ at large r_1 and small r_2, and vice versa, emphasized most forcefully the 'in–out' feature found in $\Delta D(r_1)$.

Correlation produces changes in the angular and radial expectation properties for H^- which are massive by comparison with the findings for $Z \geqslant 2$. Ratios of statistical correlation coefficients, each formulated from specific expectation values, proved to be highly informative. For every system except H^-, the ratio of the outer to the inner effect for both the radial and angular measures of correlation are virtually identical. Further, although statistical coefficients indicate that angular correlation increases in *relative* importance as Z increases, they also suggest that the major influence on the two-particle distribution arises from radial correlation.

Finally, the dramatic changes created by each component of correlation for H^- set it apart from He and the positive ions.

References

Audebert P, Geindre J P, Gauthier J C and Popovics C 1984 *Phys. Rev.* A **30** 768
Banyard K E 1990 *J. Phys. B: At. Mol. Opt. Phys.* **23** 777
Banyard K E and Ellis D J 1972 *Mol. Phys.* **24** 1291
—— 1975 *J. Phys. B: At. Mol. Phys.* **8** 2311
Banyard K E, Keeble D R T and Drake G W F 1992 *J. Phys. B: At. Mol. Opt. Phys.* **25** 3405
Banyard K E and Mobbs R J 1981 *J. Chem. Phys.* **75** 3433
Chen Z, Bao C G and Lin C D 1992 *J. Phys. B: At. Mol. Opt. Phys.* **25** 61
Dmitrieva I K and Plindov G I 1988 *J. Phys. B: At. Mol. Opt. Phys.* **21** 3055
Drake G W F 1986 (unpublished calculations based on Drake G W F 1970 *Phys. Rev. Lett.* **24** 126)
Ezra G S and Berry R S 1983 *Phys. Rev.* A **28** 1974
Froese-Fischer C 1987 *Comput. Phys. Commun.* **43** 355
Herrick D R and Kellman M E 1980 *Phys. Rev.* A **21** 418; *Phys. Rev.* A **22** 1517
Ivanov P B 1992 *J. Phys. B: At. Mol. Opt. Phys.* **25** 23
Karim K R and Bhalla C P 1988 *Phys. Rev.* A **37** 1507
Krause J L, Morgan J D III and Berry R S 1987 *Phys. Rev.* A **35** 3189
Kutzelnigg W, Del Re G and Berthier G 1968 *Phys. Rev.* **172** 49
Nicolaides C A, Makri N and Komninos Y 1987 *J. Phys. B: At. Mol. Phys.* **20** 4963
Ojha P C and Berry R S 1987 *Phys. Rev.* A **36** 1575
Rau A P P and Molina Q 1989 *J. Phys. B: At. Mol. Opt. Phys.* **22** 189

Rehmus P, Kellman M E and Berry R S 1978 *Chem. Phys.* **31** 239
Sinanoğlu O and Herrick D R 1975 *J. Chem. Phys.* **62** 886
Thakkar A J 1987 *Density Matrices and Density Functionals* ed R M Erdahl and V H Smith Jr (Dordrecht: Reidel) p 553
Tweed R J 1973 *J. Phys. B: At. Mol. Phys.* **6** 770
Weiss A W 1961 *Phys. Rev.* **122** 1826
Westerveld W B, Kets F B, Heideman H G M and van Eck J 1979 *J. Phys. B: At. Mol. Phys.* **12** 2575
Youngman P K and Banyard K E 1987 *J. Phys. B: At. Mol. Phys.* **20** 3313